

Physical Layer Security of Terahertz and Infrared Wireless Links in Atmospheric Turbulence

Yu Mei, Xiao Zhang, Rong Wang, Jianping An, Jianjun Ma*

School of Information and Electronics, Beijing Institute of Technology, Beijing 100081, China

* Correspondence: jianjun_ma@bit.edu.cn

Abstract

The future applications of terahertz (THz) wireless communication require investigations on link secrecy performance in all kinds of atmospheric conditions, including fog, snow, rain and atmospheric turbulence. Here, we present theoretical studies on physical layer security of point-to-point THz and infrared (IR) wireless links in atmospheric turbulence with a potential eavesdropper outside of the link path. Attenuations due to turbulence, gaseous absorption and beam divergence are included in the model to predict the propagation of both links. Secrecy capacity and outage probability of the THz links are calculated and compared with that of an IR (1550 nm) link. Dependences of link security on eavesdropper's position, atmospheric visibility, turbulence strength and intended data transmission rate are also presented and analyzed. We find that the THz link owns higher security at physical layer than the IR link.

Keywords: Terahertz wireless communications, infrared wireless communications, physical layer security, atmospheric turbulence, scattering

1. Introduction

Terahertz (THz) communication technique is widely considered as a promising candidate for the next generation of wireless networks due to its large data capacity and high security [1, 2], which corresponds to its advantages of wider bandwidth and higher beam directionality when compared with present radio frequencies (RF) and millimeter waves [3, 4]. It could also be a solution to provide reliable data transmission in some special application scenarios, such as in rain, snow, dust and atmospheric turbulence, when a wireless link at higher frequencies (such as infrared) is prohibited or restricted. Su *et. al.* [5, 6] compared link performance of a 625 GHz link and an IR (1550 nm) link in fog cloud and dust cloud, and proved that the THz link owns much better performance due to a small degradation it suffered. Ma *et. al.* [7] repeated the measurements in atmospheric turbulence and also observed a much lower link degradation in THz link due to the negligible signal loss by scattering it suffered.

Unlike wire communications, the broadcasting nature of wireless link makes it to be vulnerable to attacks at physical layer. One alternative solution for that is employing carrier beams with higher directionality to achieve higher security at physical layer [8]. A point-to-point link with carriers at and above THz frequencies is confirmed to provide an additional layer of security when an eavesdropper appears between two legitimate peers [1] due to its inherent narrower beam width compared to the almost broadcast nature of RF signals [9]. This leads to a high directionality and makes it much harder and even impossible to intercept the signals. However, if we consider a visible and/or IR link in clear weather, an even much higher link security would be achieved [10-12] because of its higher directionality than THz beams.

In this work, considering the smaller link degradation of THz links by scattering in atmospheric turbulence and higher security of IR links due to its high directionality in clear weather, we propose to study the secrecy performance of both links in atmospheric turbulence and find out the influencing mechanism of scattering by turbulence and inherent beam directionality. This has never been investigated before, but a comprehensive study on this topic is definitely required for the future applications of THz and even IR wireless communications.

2. Physical Characteristics of Atmospheric Turbulence

When a THz beam propagates in outside scenarios, it suffers significant absorption by water

vapor and other gases (such as oxygen) [13, 14], and also attenuation by atmospheric turbulence even in rain [15] when wind velocity reaches to one point (the critical Reynolds number equals the normal air flow [16]) where turbulence generated. Atmospheric turbulence is caused by spatial and temporal temperature inhomogeneities in air [17, 18] and is usually regarded as a large amount of air pockets with varying sizes (between a small scale size l_0 and a larger scale size L_0) and temperatures. As shown in Fig. 1(a), these air pockets can act like prisms with different refractive indices and will scatter the beam when it propagates through the turbulence. Then random fluctuation of the signal power and phasefront distortion occur spatially and temporally [19], and further degrade the link performance with lower or higher modulation formats [20, 21]. So, for long paths ($\geq 1\text{km}$) being parallel or near to the ground, scattering by atmospheric turbulence can lead to a time-varying fading effect on wireless link in the order of milliseconds [22, 23].

However, evaluation and characterization of atmospheric turbulence based on theories are very challenging and complex, because the observable atmospheric channel quantities such as wind velocity, temperature, and pressure are mixed and behave in a nonlinear fashion. Therefore, it should be characterized based on statistical distributions. Log-normal distribution model, gamma-gamma model, K-distribution model and negative exponential distribution model are usually considered for the characterization of the atmospheric turbulence and induced signal fluctuation [24]. But none of them is suitable for all the turbulence conditions due to the non-stationary nature of turbulence. Predictions by the log-normal model in weak turbulence match well with experimental measurements in [7]. This model would also be employed in this work for stochastic characteristic of channel fading in weak turbulence.

There have been several models developed to estimate the average attenuation caused only by turbulence. Rytov Method starts on the basis of Rytov's analysis without receiver aperture considered [25]. Andrew's Method is derived on the basis of a detailed mathematical analysis of atmospheric turbulence presented by Larry C. Andrews [25]. Kruse *et. al.* [26] derived a method which has served a long time to the infrared and far-infrared communication community as the only model providing a wavelength dependent between the atmospheric turbulence and the attenuation coefficient. It was first developed for fog attenuation modeling, and could also be used for atmospheric turbulence [27] as

$$\alpha_t = \frac{3.91}{V} \left(\frac{\lambda}{0.55} \right)^{-p} \quad (1)$$

here, λ in [μm] is incident wavelength. V in [m] is atmospheric visibility which is defined as a distance where the $0.55\mu\text{m}$ collimated light beam is attenuated to a fraction (5% or 2%) of an original power. p is the size distribution of scattering air pockets and can obtain by a piecewise function of V in several models. Kruse model is firstly proposed in [28] to preset the relation between both and can only be used when visibility $V \leq 1\text{km}$ [29]. Then, Kim modified this model [30] and make it to be available over full visibility range as

$$\begin{aligned} p &= 1.6 & V &> 50 \text{ km} \\ &= 1.3 & 6\text{km} < V \leq 50 \text{ km} \\ &= 0.34 + 1.6V & 1\text{km} < V \leq 6\text{km} \\ &= V - 0.5 & 0.5\text{km} < V \leq 1\text{km} \\ &= 0 & V \leq 0.5\text{km} \end{aligned} \quad (2)$$

which would be employed for the prediction of link performance with visibility $V \leq 1\text{km}$ in this work.

3. Secrecy capacity

3.1 Calculation model

Here, we assume there is a point-to-point outdoor THz link and the configuration is shown in Fig.1 (b). A transmitter (Alice) sends information to a legitimate receiver (Bob) by a line-of-sight (LOS) link which suffers absorption and scattering in atmospheric turbulence. Meanwhile, an eavesdropper (Eve) exists outside but near the link path and aims to capture the information through a non-line-of-sight (NLOS) channel scattered away from the legitimate (LOS) path. The link distance d is set at $d=1\text{km}$ in all the calculations, and so, positions of Alice and Bob are always fixed. Eve can change its position and adjust its pointing direction to obtain optimal received signal.

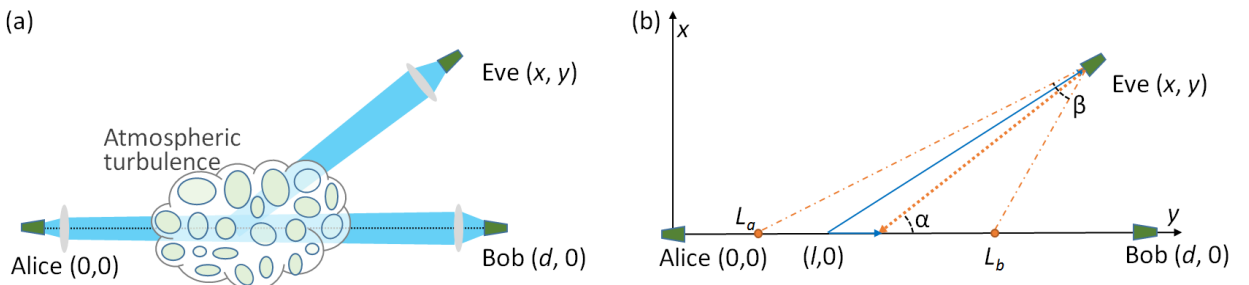


Figure 1 (a) Geographic of the point-to-point THz link with a security attacker (Eve) in atmospheric turbulence; (b) Coordinate system of the legitimate (LOS) and eavesdropping (NLOS) links.

In the presence of atmospheric turbulence, the LOS link suffers atmospheric attenuation G_F and divergence attenuation $G_D = 4A/(\pi d^2 \alpha_A^2)$ with α_A as the full divergence angle of Alice and A as the effective receiving area of Bob. The atmospheric attenuation consists of two parts: attenuation only by turbulence (with coefficient as α_t) and gaseous attenuation (with coefficient as α_g) [31] by air. The latter one is commonly described as the sum of spectral absorption link of oxygen, water vapor and a water vapor continuum component [24]. So the atmospheric attenuation coefficient is $\alpha_{atm} = \alpha_t + \alpha_g$ and the atmospheric attenuation can be obtained by $G_F = \exp(-\alpha_{atm}d)$.

Combining both atmospheric attenuation and divergence attenuation, we can get the total LOS link gain as

$$G_{\text{LOS}} = G_F G_D = \frac{4Ae^{-\alpha_{atm}d}}{\pi d^2 \alpha_A^2} \quad (3)$$

To obtain the link gain of the eavesdropping (NLOS) link achieved by scattering, a widely used model, called single-scattering model [32, 33], is employed. In the link geometry shown in Fig. 1(b), we set Alice at the origin of the coordinate $(0, 0)$, Bob at $(d, 0)$ and Eve at (x, y) . The signal is transmitted along the positive direction of the x -axis between Alice and Bob. The NLOS link gain G_{NLOS} can be obtained as in [34] by

$$G_{\text{NLOS}} = \int_{L_a}^{L_b} \Omega(l) p(\mu) \alpha_{atm} e^{-\alpha_{atm}[l + \sqrt{(x-l)^2 + y^2}]} dl \quad (4)$$

with integral variable l as the signal transmission distance before scattering occurs. The lower bound L_a and upper bound L_b , expressed as

$$L_b = \min \left\{ \max \left\{ x - \frac{y}{\tan(\alpha - \beta/2)}, 0 \right\}, d \right\} \quad (5)$$

$$L_e = \min \left\{ \max \left\{ x - \frac{y}{\tan(\alpha + \beta/2)}, 0 \right\}, d \right\} \quad (6)$$

divide the scattering region. Here, α represents the scattering angle of Eve, which means the point angle from scattering point $(l, 0)$ to Eve (x, y) . The optimal scattering angle, corresponding to maximum NLOS link gain, can be expressed as $\alpha^* = \arctan(y/x) + \beta/2$ for $\alpha < \pi/2 - \beta/2$ [27]. The parameter β represents full angle of field of sight (FOV) of Bob. $\Omega(l)$ denotes the solid angle from receiving area to the scattering point

$$\Omega(l) = \frac{A}{\left[(x-l)^2 + y^2\right]^{3/2}} \frac{(x-l) + y \tan \alpha}{\sqrt{1 + \tan^2 \alpha}} \quad (7)$$

The factor $p(\mu)$ can be expressed as

$$p(\mu) = \frac{1-g^2}{4\pi} \left[\frac{1}{(1+g^2-2g\mu)^{3/2}} + f \frac{3\mu^2-1}{2(1+g^2)^{3/2}} \right] \quad (8)$$

when generalized Henyey-Greenstein function is adopted, and it is defined as scattering phase function indicating the probability distribution of scattering angle. $\mu = (x-l)/\sqrt{(x-l)^2 + y^2}$ represents the cosine of scattering angle in $(l, 0)$ with g as an asymmetry factor related to wavelength, scattering particle radius and refractive index [35].

3.2 Secrecy performance analysis

In the calculation, a 300 GHz link and a 1550 nm link are considered and assumed to be collimated with the same beam width. The FOV angles of Eve for both links are set to be 30° and the receiving areas for Bob and Eve are all 1cm^2 . To calculate the gaseous attenuation α_g , we set temperature $T = 25^\circ\text{C}$, pressure $P = 1013 \text{ hPa}$, and relative humidity $\text{RH} = 60\%$, which are all chosen in the following calculations. When Eve is set at a position of $(200\text{m}, 10\text{m})$, the link gain is calculated and shown in Fig. 2. Solid lines represent the evolution of link gain G_{LOS} for the LOS link as a function of atmospheric visibility V . It increases as the increasing of atmospheric visibility due to the decreasing of attenuation by turbulence α_t , which reaches to 0 when $V > 1\text{km}$ for the THz link and when $V > 3\text{km}$ for the IR link. This indicates that the THz link suffers less attenuation by the turbulence. The dashed lines represent the variation of NLOS link gain G_{NLOS} , which is larger than the LOS link gain G_{LOS} first due to the serious scattering by strong atmospheric turbulence. Then it decreases gradually with the increasing of visibility because of the decreasing of atmospheric attenuation. When $V = 0.5\text{km}$, an intersection between both gains comes for the THz link, Bob and Eve can obtain the same link gain and the secrecy risk comes for the THz link. For the IR link, that comes when $V = 0.6\text{km}$. This indicates that the THz link is less vulnerable to attack due to turbulence.

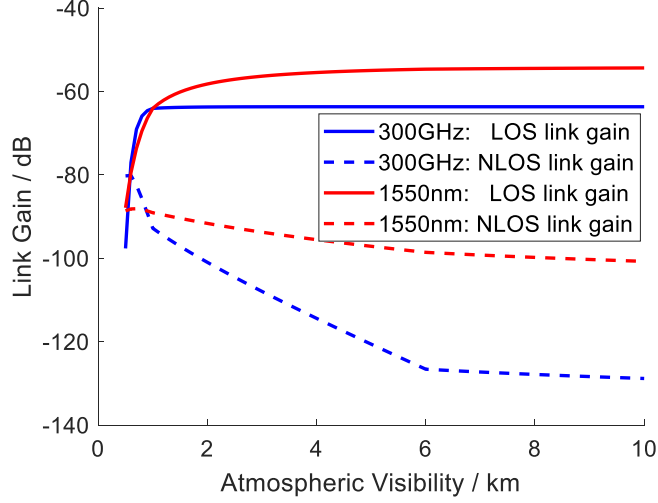


Figure 2 Link gain of the legitimate (LOS) and eavesdropping (NLOS) channels with respect to atmospheric visibility V . (Temperature $T = 25^{\circ}\text{C}$, Pressure $P = 1013 \text{ hPa}$, and relative humidity $\text{RH} = 60\%$).

Secrecy capacity is defined as the maximum data rate from Alice to Bob when perfect secrecy performance is maintained [36] and can be expressed as

$$C_s = [I(X;Y) - I(X;Z)]^+ \quad (9)$$

with $[x]^+ = \max\{0, x\}$ indicating that the secrecy capacity can never be less than 0. Parameters X , Y and Z represents the signals of the Alice, Bob and Eve, respectively. $I(X;Y)$ and $I(X;Z)$ denote the mutual information of LOS and NLOS links [37], respectively, and can be expressed as

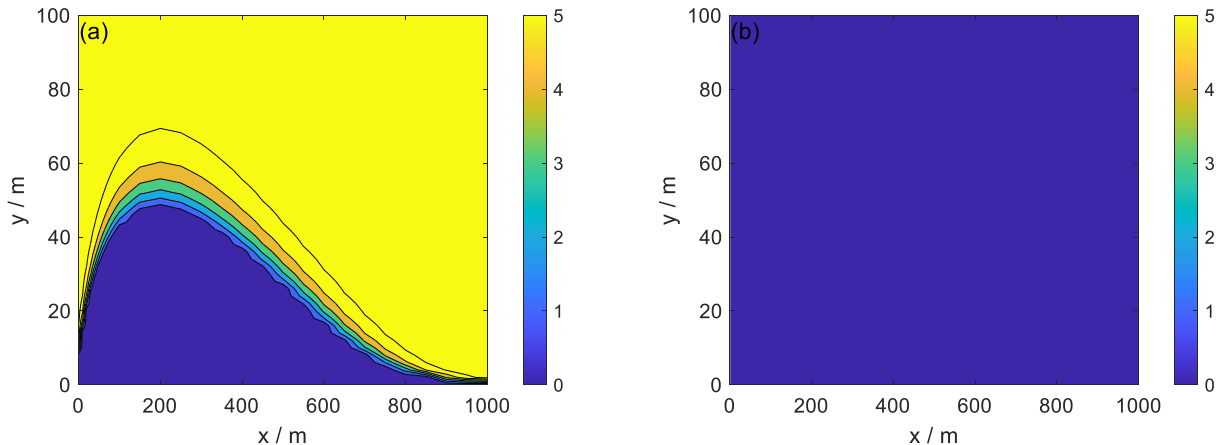
$$I(X;Y) = q(\lambda_L + \lambda_b) \log(\lambda_L + \lambda_b) + \lambda_b \log(\lambda_b) - (q\lambda_L + \lambda_b) \log(q\lambda_L + \lambda_b) \quad (10)$$

$$I(X;Z) = q(\lambda_N + \lambda_b) \log(\lambda_N + \lambda_b) + \lambda_b \log(\lambda_b) - (q\lambda_N + \lambda_b) \log(q\lambda_N + \lambda_b) \quad (11)$$

when an on-off keying modulation format with a duty cycle q and a Poisson distribution, which is a common assumption for stochastic links, are assumed. $\lambda_L = \tau\eta G_{\text{LOS}} P/E_p$ and $\lambda_N = \tau\eta G_{\text{NLOS}} P/E_p$ represent the mean numbers of detected photoelectrons of signal component in each slot for the LOS and NLOS links, respectively. P is the output power from Alice and η is the receiver efficiency, which are identical for Bob and Eve and are always set at $P = 1 \text{ W}$, $\eta = 0.1$ in the calculation. E_p is the energy of one THz or IR photon and τ is integration time of the receivers of Bob and Eve. λ_b represent the mean number of detected photoelectrons of background radiation component in each slot. In experimental measurement, the infrared radiation (sometimes called laser beam) is converted to electrical power by photovoltaics; and the THz radiation is converted to direct current (DC)

electrical power using a rectifying diode and an antenna. Both methods are based on the conversion of photoelectron to current. So here, we take the photoelectron in consideration in our calculation and the signal to noise ratio (SNR) of receiver can be obtained by dividing λ_L by λ_b .

The secrecy capacity distributions with respect to arbitrary positions of Eve are calculated and shown in Fig. 3(a) and (b) when the atmospheric visibility $V = 0.5\text{km}$. The color bars on the right denote the safe transmission rates in Gbps, which increases gradually as the color changes from blue to yellow. In Fig. 3(a) for the THz link, the dark blue region represents $C_s = 0$, which means the secure transmission cannot be guaranteed if Eve is located in this region. We could call it as insure region. However, in Fig. 3(b) for the IR link, the whole region is in dark blue and insecure due to the higher scattering suffered by the IR link. For the THz wave at 300 GHz, its wavelength is around 650 times larger than the IR wavelength. This makes the THz link suffers less signal scattering effect by the atmospheric turbulence, which has been confirmed in experimental measurements [7]. In Fig. 3(c) and (d), when the visibility is increased to $V = 0.6\text{km}$, the secrecy of both links are increased. The insecure region of the THz link disappears and the safe data transmission rate of the IR link could never be 0 in the whole region.



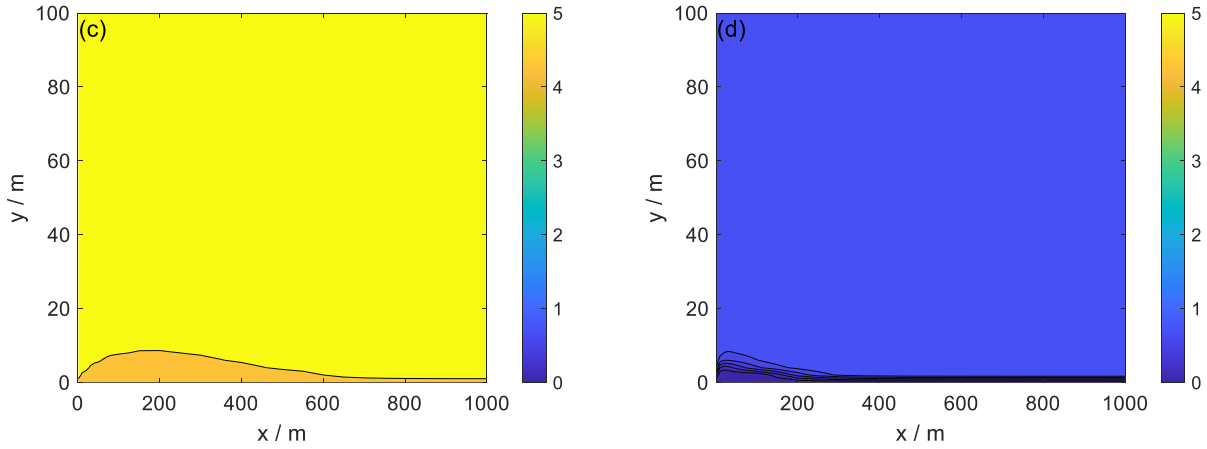


Figure 3 Secrecy capacity distribution for 2-D positions of Eve when (a) 300 GHz link with $V = 0.5$ km, (b) 1550 nm link with $V = 0.5$ km, (c) 300 GHz link with $V = 0.6$ km and (d) 1550 nm link with $V = 0.6$ km are chosen.

If we consider commercial products for the generation of THz and IR signals, the divergence angle should be 10° for THz link [38] and 15 mrad for IR link [39]. Then we do the same calculation as in Fig. 3 and set a larger visibility $V = 0.7$ km to reduce the atmospheric attenuation and increase link gain. The secrecy capacity distribution is plotted in Fig. 4. In Fig. 4(a), the insecure region (dark blue region) moves closer to Bob when compared with Fig. 3(a) or (c). We attribute this to the larger coverage of the THz beam due to its larger divergence angle we assumed. The insecure region of the IR link in Fig. 4(b) is reduced and the safe transmission rate can be above 0, but it is still much below that of the THz link.

To further see the variation of secrecy performance at different carrier frequencies, we choose 100 GHz and 200 GHz links for calculation which are not that far away from the 300 GHz at the electromagnetic spectrum. Under the same parameter settings (such as divergence angle, visibility and link distance) with Fig. 4(a) , the secrecy capacity distributions of both links are plotted in Fig. 4(c) and (d). From the comparison of Fig. 4(a), (c) and (d), we can see that the 100 GHz and 200 GHz links own the higher security corresponding to smaller insecure region. And the area of the region becomes larger for higher frequencies due to more serious scattering and higher gaseous attenuation it suffered. So if we hope to increase the security of a THz wireless link, small divergence angle and/or carrier frequency should be efficient methods.

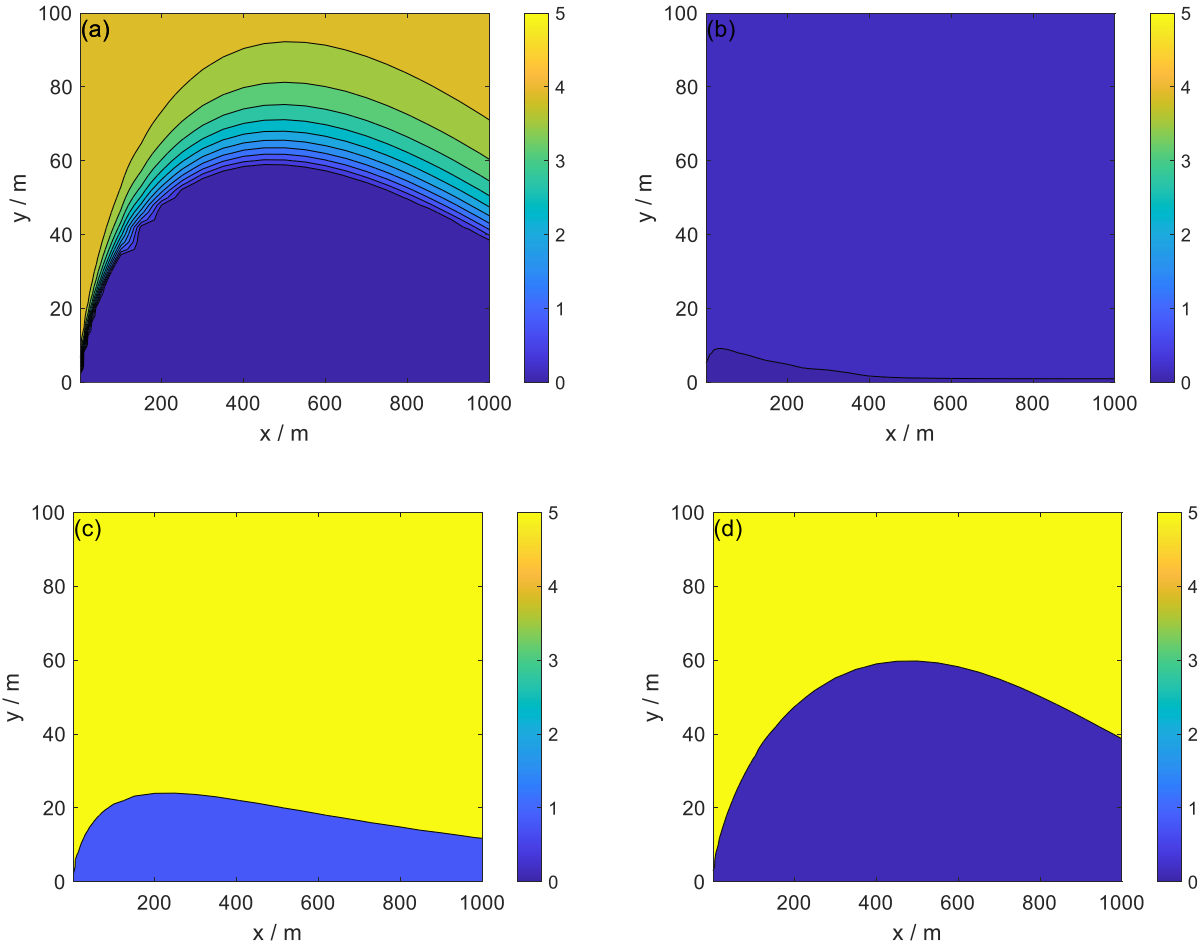


Figure 4 Secrecy capacity distribution for 2-D positions of Eve when (a) 300 GHz, (b) 1550 nm, (c) 100 GHz and (d) 200 GHz links are chosen with visibility $V = 0.7$ km.

4. Outage probability

4.1 Calculation model

In the calculation of secrecy capacity in Section 3, only averaged atmospheric attenuation can be calculated in the theoretical model and so the link gain is an averaged value also. But this is not the actual situation. The received signal power and link gain should fluctuate spatially and temporally due to the scattering induced scintillation effect along the link paths [40]. So in this section, we introduce random fluctuations and a stochastic characterization to the LOS link, while the NLOS link gain is still considered as a constant due to the fact that the scattered signal power received by Eve could never be comparable to or larger than the LOS gain. Otherwise, the LOS link would fail due to a serious power loss. The NLOS link gain should be always much smaller than the LOS link gain

and random fluctuations of it would have almost no influence on the secrecy performance of the whole link.

To depict the signal distribution in weak turbulence, the log-normal model is regarded a perfect tool for the theoretical model [41] and secrecy outage probability is employed here as a probabilistic indicator to characterize the link secrecy. It is defined as the probability that the instantaneous secrecy capacity falls below a target rate which can be expressed as [42]

$$P_0(R) = P_r \{C_s < R\} \quad (12)$$

with R is the given minimal secure transmission rate ($R \geq 0$). It is usually regarded as the probability of existence of a secure link. Eq. (12) can be rewritten as

$$P_o(R) = \int_{C_s \leq R} f_{\text{LOS}}(G_{\text{LOS}}) dG_{\text{LOS}} = \int_0^G f_{\text{LOS}}(G_{\text{LOS}}) dG_{\text{LOS}} \quad (13)$$

with G as the solution of $C_s = R$ and G_{LOS} as the instantaneous LOS link gain in this section. The probability density function of the instantaneous LOS link gain can then be expressed by [16]

$$f_{\text{LOS}}(G_{\text{LOS}}) = \frac{1}{G_L \sqrt{2\pi\sigma_r^2}} \exp \left[-\frac{\left(\log(G_{\text{LOS}}/\bar{G}_{\text{LOS}}) - \langle \log(G_{\text{LOS}}/\bar{G}_{\text{LOS}}) \rangle \right)^2}{2\sigma_r^2} \right] \quad (14)$$

Here, \bar{G}_{LOS} is the mean value of random variable G_{LOS} . $\langle \log(G_{\text{LOS}}/\bar{G}_{\text{LOS}}) \rangle$ is the mean value of $\log(G_{\text{LOS}}/\bar{G}_{\text{LOS}})$ and can be written as $\langle \log(G_{\text{LOS}}/\bar{G}_{\text{LOS}}) \rangle = -\sigma_r^2/2$. The parameter σ_r^2 represents the variance of $\log(G_{\text{LOS}})$. In the presence of atmosphere turbulence, σ_r^2 is defined as Rytov variance characterizing the strength of turbulence over a transmission link employing an infinite plane wave. $\sigma_r^2 = 1.23C_n^2k^{7/6}d^{11/6}$ is a function of atmosphere refraction structure parameter C_n^2 , the wave number $k = 2\pi/\lambda$, and the link distance d . In terms of this parameter, we choose $\sigma_r^2 < 1$ as the characterization of weak turbulence [25].

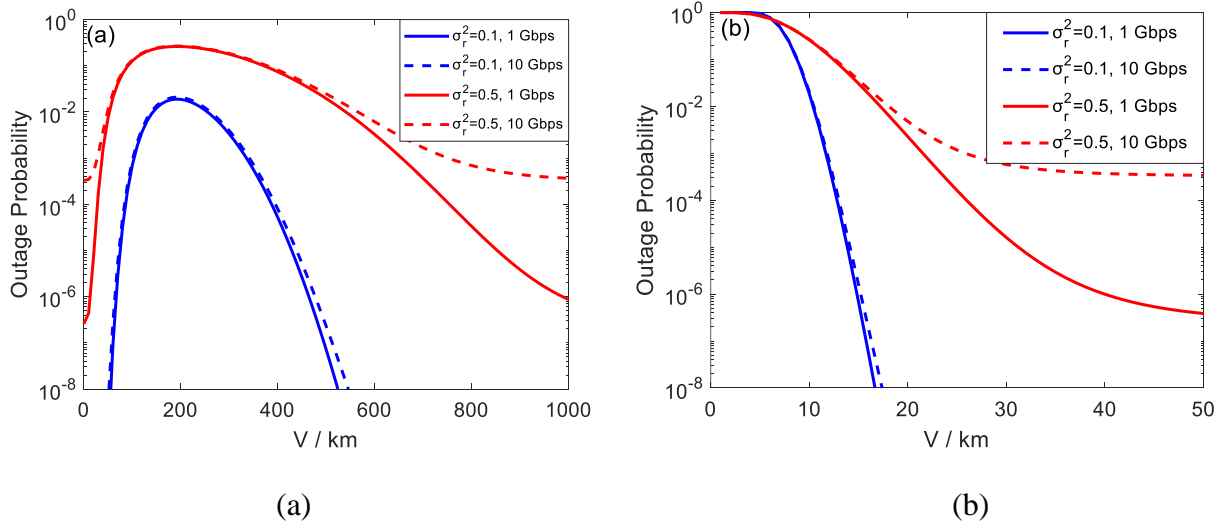
4.2 Secrecy performance analysis

Under the settings of $V = 0.6$ km, $d = 1$ km and SNR=3dB of the receiver, the variation of outage probability of the 300 GHz link is calculated and plotted in Fig.5 with turbulence strength and intended transmission data rate are considered, which could also influence the outage probability. The Rytov variance is set around 0.1 and 0.5 belonging to weak turbulence for the THz link. Fig. 5(a) plots the evolution of outage probability with respect to the position of Eve on x -axis along $y = 15$ m. For a

given turbulence strength and transmission data rate, with the increasing of x value, the outage probability increases significantly first and reaches maximum when x -value is around 200m; then it decreases always. This trend is consistent with the performance plotted in Fig. 3(a) and (c) where a collimated beam is considered. When Eve is near Alice, the scattered power could not be enough for decoding, and when Eve is near Bob, the scattering cannot be enough also due to the narrow beam width and large gaseous attenuation.

In Fig. 5(b), the outage probability is plotted versus the position of Eve on y -axis along $x = 200$ m. With the increasing of y value, the outage probability decreases remarkably because of the increasing of gaseous absorption. Fig. 5(c) shows the evolution of outage probability with respect to atmospheric visibility when Eve is positioned at (500m, 5m). The outage probability decreases significantly with the increasing of visibility due to the decreasing of scattering effect and corresponding eavesdropping link gain. Fig. 5(d) shows that the outage probability is very sensitive to the carrier frequency and the THz link could be definitely insecure when a 500 GHz frequency employed under Rytov variance at $\sigma_r^2 = 0.5$ and intended data rate $R = 10$ Gbps.

When we look back to the first three plots in Fig. 5, by comparing the blue and red curves, we can see that the outage probability increases dramatically under stronger turbulence; by comparing the solid and dashed curves, we can find that larger intended data rate could reduce the link security due to the larger SNR the link required.



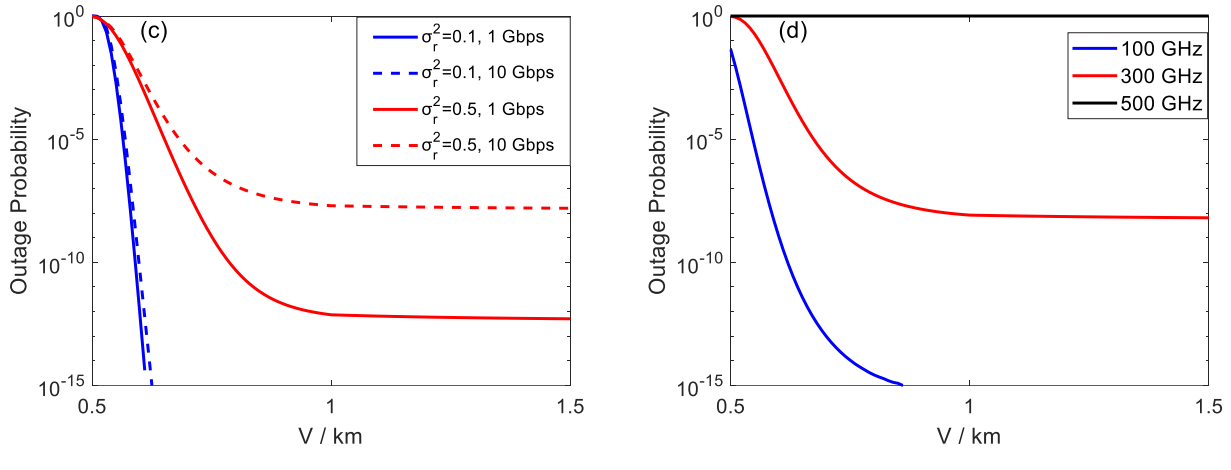


Figure 5 Variation of outage probability with respect to Eve's position on (a) x-axis and (b) y-axis; Variation of outage probability versus atmospheric visibility under (c) different turbulence strengths and intended data rates and (d) carrier frequencies.

Conclusions

In this paper, we investigate the secrecy performance of point-to-point THz and IR links in atmospheric turbulence when an eavesdropper locates outside of the link path. A theoretical model combining atmospheric attenuation, scattering theories and stochastic models are proposed to predict the secrecy capacity distribution and outage probability. The calculation results show that, compared with an IR link at 1550nm, the THz link at 300 GHz own higher security even with a much larger divergence angle at transmitter side being assumed. At THz range, larger insecure regions and larger outage probabilities are also observed at higher THz frequencies due to the serious link degradations caused by turbulence induced scattering effect. And the security at physical layer becomes even worse when turbulence strength and/or transmitted data rate increase.

Funding Information

This research was supported by Beijing Institute of Technology Research Fund Program for Young Scholars (No. 3050011181910).

References

- [1] J. Ma, R. Shrestha, J. Adelberg, C.-Y. Yeh, Z. Hossain, E. Knightly, *et al.*, "Security and eavesdropping in terahertz wireless links," *Nature*, vol. 563, p. 89, Oct 15 2018.
- [2] X. Li, J. Yu, L. Zhao, K. Wang, C. Wang, M. Zhao, *et al.*, "1-Tb/s Millimeter-Wave Signal Wireless Delivery at D-Band," *Journal of Lightwave Technology*, vol. 37, pp. 196-204, 2019.
- [3] R. Singh, W. Lehr, D. Sicker, and K. M. S. Huq, "Beyond 5G: The Role of THz Spectrum," *Available at SSRN 3426810*, 2019.
- [4] J. F. O'Hara, S. Ekin, W. Choi, and I. Song, "A Perspective on Terahertz Next-Generation Wireless Communications," *Technologies*, vol. 7, p. 43, 2019.
- [5] K. Su, L. Moeller, R. B. Barat, and J. F. Federici, "Experimental comparison of terahertz and infrared data signal attenuation in dust clouds," *Journal of the Optical Society of America a-Optics Image Science and Vision*, vol. 29, pp. 2360-2366, Nov 2012.
- [6] K. Su, L. Moeller, R. B. Barat, and J. F. Federici, "Experimental comparison of performance degradation from terahertz and infrared wireless links in fog," *Journal of the Optical Society of America a-Optics Image Science and Vision*, vol. 29, pp. 179-184, Feb 2012.
- [7] J. Ma, L. Moeller, and J. F. Federici, "Experimental Comparison of Terahertz and Infrared Signaling in Controlled Atmospheric Turbulence," *Journal of Infrared, Millimeter and Terahertz Waves*, vol. 36, pp. 130-143, Feb 2015.
- [8] Y. Liu, H.-H. Chen, and L. Wang, "Physical Layer Security for Next Generation Wireless Networks: Theories, Technologies, and Challenges," *IEEE Communications Surveys & Tutorials*, vol. 19, pp. 347-376, 2017.
- [9] D. Steinmetzer, J. Chen, J. Classen, E. Knightly, and M. Hollick, "Eavesdropping with periscopes: Experimental security analysis of highly directional millimeter waves," presented at the 2015 IEEE Conference on Communications and Network Security (CNS), 2015.
- [10] T. L. Wang and I. B. Djordjevic, "Physical-layer security in free-space optical communications using Bessel-Gaussian beams," presented at the IEEE Photonics Conference (IPC), 2018.
- [11] A. Mostafa and L. Lampe, "Physical-layer security for indoor visible light communications," presented at the IEEE International Conference on Communications (ICC), 2014.
- [12] X. Sun and I. B. Djordjevic, "Physical-Layer Security in Orbital Angular Momentum Multiplexing Free-Space Optical Communications," *IEEE Photonics Journal*, vol. 8, pp. 1-10, 2016.
- [13] Y. Li, W. Jin, C. Liu, X. Wang, Y. Ding, X. Shi, *et al.*, "Simulation and analysis of atmospheric transmission performance in airborne Terahertz communication," presented at the Fourth Seminar on Novel Optoelectronic Detection Technology and Application, Nanjing, China, 2017.
- [14] J. Ma, R. Shrestha, L. Moeller, and D. M. Mittleman, "Invited Article: Channel performance for indoor and outdoor terahertz wireless links," *APL Photonics*, vol. 3, p. 12, 2018.
- [15] A. Hirata, H. Takahashi, T. Kosugi, K. Murata, K. Naoya, and Y. Kado, "Rain attenuation statistics for a 120-GHz-band wireless link," presented at the 2009 IEEE MTT-S International Microwave Symposium Digest, 2009.
- [16] L. C. Andrews and R. L. Phillips, *Laser beam propagation through random media*. Bellingham, Washington USA: SPIE Press, 2005.
- [17] Z. Ghassemlooy, W. Popoola, and S. Rajbhandari, *Optical wireless communications: system and channel modelling with Matlab®*: CRC Press, 2012.
- [18] A. Labeyrie, S. G. Lipson, and P. Nisenson, *An introduction to optical stellar interferometry*: Cambridge University Press, 2006.
- [19] H. E. Nistazakis, T. A. Tsiftsis, and G. S. Tombras, "Performance analysis of free-space optical communication

systems over atmospheric turbulence channels," *IET Communications*, vol. 3, p. 1402, 2009.

[20] T. Nagatsuma, G. Ducournau, and C. C. Renaud, "Advances in terahertz communications accelerated by photonics," *Nature Photonics*, vol. 10, pp. 371-379, 2016.

[21] J. Federici and L. Moeller, "Review of terahertz and subterahertz wireless communications," *Journal of Applied Physics*, vol. 107, Jun 1 2010.

[22] M. O. Zaatari, "Wireless Optical Communications Systems in Enterprise Networks," *The Telecommunications Review*, pp. 49-57, 2003.

[23] G. P. Berman, A. R. Bishop, B. M. Chernobrod, D. C. Nguyen, and V. N. Gorshkov., "Suppression of intensity fluctuations in free space high-speed optical communication based on spectral encoding of a partially coherent beam," *Optics Communications*, vol. 280, pp. 2264-2270 2007.

[24] J. Ma, "Terahertz wireless communication through atmospheric turbulence and rain," Ph. D, School of Physics, New Jersey Institute of Technology, 2016.

[25] L. C. Andrews, *Field Guide to Atmospheric Optics*: SPIE Publications, 2004.

[26] P. W. Kruse, L. D. McLaughlin, and R. B. Ricklin, *Elements of Infrared Technology: Generation, Transmission and Detection*. New York: John Wiley & Sons, 1962.

[27] D. Zou and Z. Xu, "Information Security Risks Outside the Laser Beam in Terrestrial Free-Space Optical Communication," *IEEE Photonics Journal*, vol. 8, pp. 1-9, 2016.

[28] T. S. Rappaport, *Wireless Communications: Principles and Practice*. Upper Saddle River, NJ: Prentice Hall, 2002.

[29] I. I. Kim, B. McArthur, and E. J. Korevaar., "Comparison of laser beam propagation at 785 nm and 1550 nm in fog and haze for optical wireless communications," presented at the Optical Wireless Communications III, International Society for Optics and Photonics, 2001.

[30] I. I. Kim, B. McArthur, and E. J. Korevaar, "Comparison of laser beam propagation at 785 nm and 1550 nm in fog and haze for optical wireless communications," *Proc Spie*, vol. 4214, pp. 26-37, 2001.

[31] M. Taherkhani, Z. G. Kashani, and R. A. Sadeghzadeh, "On the performance of THz wireless LOS links through random turbulence channels," *Nano Communication Networks*, vol. 23, p. 100282, 2020.

[32] H. Xiao, Y. Zuo, J. Wu, Y. Li, and J. Lin, "Non-line-of-sight ultraviolet single-scatter propagation model in random turbulent medium," *Optics Letters*, vol. 38, p. 3366, 2013.

[33] M. R. Luettgen, J. H. Shapiro, and D. M. Reilly, "Non-line-of-sight single-scatter propagation model," *Journal of the Optical Society of America A*, vol. 8, pp. 1964-1972, 1991.

[34] D. Zou and Z. Xu, "Information Security Risks Outside the Laser Beam in Terrestrial Free-Space Optical Communication," *IEEE Photonics Journal*, vol. PP, pp. 1-1, 2016.

[35] C. Xu, H. Zhang, and J. Cheng, "Effects of haze particles and fog droplets on NLOS ultraviolet communication channels," *Opt Express*, vol. 23, pp. 23259-69, Sep 7 2015.

[36] R. Bustin, R. Liu, H. Poor, and S. Shamai, "An MMSE Approach to the Secrecy Capacity of the MIMO Gaussian Wiretap Channel," *Eurasip Journal on Wireless Communications & Networking*, vol. 2009, p. 3, 2009.

[37] A. D. Wyner, "Capacity and error component for the direct detection photon channel - Paart I-II," *IEEE Transactions on Information Theory*, vol. 34, pp. 1499-1471, 1988.

[38] *VDI Feedhorn Summary*. Available:
https://vadiodes.com/VDI/pdf/VDI%20Feedhorn%20Summary%202006_05.pdf

[39] *1550nm Eye Safe Laser*. Available: <https://www.beamqus.com/product/1550nm-eye-safe-laser/>

[40] A. Alkholidi and K. Altowij, "Effect of Clear Atmospheric Turbulence on Quality of Free Space Optical Communications in Western Asia," 2012.

[41] X. Tang, S. Rajbhandari, W. O. Popoola, Z. Ghassemlooy, and G. Kandus, "Performance of BPSK Subcarrier

Intensity Modulation Free-Space Optical Communications using a Log-normal Atmospheric Turbulence Model," presented at the Symposium on Photonics & Optoelectronic (SOPO), Chengdu, China, 2010.

[42] M. Bloch, J. Barros, M. Rodrigues, and S. McLaughlin, "Wireless information-theoretic security," *IEEE Transactions on Information Theory*, vol. 54, pp. 2515-2534, 2008.